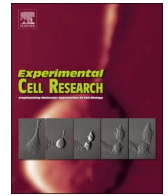




Contents lists available at ScienceDirect

Experimental Cell Research

journal homepage: www.elsevier.com/locate/yexcr

MicroRNA-21 promotes wound healing via the Smad7-Smad2/3-Elastin pathway

Xiaoyan Li^a, Lijia Guo^b, Yitong Liu^a, Yingying Su^c, Yongmei Xie^a, Juan Du^a, Songling Wang^d, Hao Wang^{c,*}, Yi Liu^{a,*}

^a Laboratory of Tissue Regeneration and Immunology and Department of Periodontics, Beijing Key Laboratory of Tooth Regeneration and Function Reconstruction, School of Stomatology, Capital Medical University, PR China

^b Department of Orthodontics School of Stomatology, Capital Medical University, PR China

^c Department of Stomatology, Beijing Tiantan Hospital, Capital Medical University, PR China

^d Salivary Gland Disease Center and Molecular Laboratory for Gene Therapy and Tooth Regeneration, School of Stomatology, Capital Medical University, PR China

ARTICLE INFO

Keywords:

Wound healing
MiR-21
GMSCs
Elastin

ABSTRACT

Wound healing is regulated by a complex network of cells, molecules, and cytokines, as well as microRNAs (miRNAs). miRNAs were confirmed to influence the wound healing process, and miR-21, an important member of the miRNA family, was also shown to regulate wound healing. The aim of the present study was to investigate the role of miR-21 in the wound healing process and the possible underlying cell signaling pathways. We isolated GMSCs from WT and miR-21-KO mouse gingiva. Flow cytometric analysis and immunocytofluorescence staining were used to identify the GMSCs acquired from WT and miR-21-KO mice. RT-PCR, western blot analysis and immunohistochemistry staining were performed to examine the expression of extracellular matrix components and key proteins of cell signaling pathways. TargetScan and pmir-RB-REPORT vectors were used to verify that Smad7 was a direct target of miR-21. Compared to WT mice, miR-21-KO mice showed slower wound healing. RT-PCR and western blot analysis indicated that Elastin expression was downregulated in miR-21-deficient samples. We confirmed that Smad7 was a direct target of miR-21. miR-21 knockout resulted in increased expression of Smad7 and impaired phosphorylation of the Smad2/3 complex. The expression of the Smad7-Smad2/3-Elastin axis in palate tissues sections acquired from WT and miR-21-KO mice showed the same trend. Based on all these results, we demonstrated that miR-21 promoted the wound healing process via the Smad7-Smad2/3-Elastin pathway.

1. Introduction

Wound healing is a very complicated process, that can be briefly divided into three stages: inflammation, extracellular matrix (ECM) deposition, and remodeling. Wound healing starts immediately after the initial lesion and lasts until complete closure of the wound and functional restitution of the tissue [1]. This process requires the integration of complex biological and molecular events and involves soluble factors, primarily coagulation factors, growth factors and cytokines. Additionally, different sources of stem cells also play a specific role in this process.

Multipotent mesenchymal stromal cells, also referred to as mesenchymal stem cells (MSCs), are known for their multipotency. MSCs are capable of homing and engrafting into damaged tissues, releasing trophic factors, secreting ECM and promoting neovascularization [2]; thus, they are an indispensable component of the wound healing

process. The biological ability of MSCs is controlled by inflammatory cytokines, growth factors, and oxidative stress, as well as microRNAs.

MicroRNAs (miRNAs or miRs) are non-coding RNAs of 21–25 nucleotides in length that regulate gene expression through translational inhibition as well as destabilization of mRNA, coordinating a broad spectrum of biological processes [3]. miR-21 is a crucial member of the miRNA family, and previous studies have confirmed the effect of miR-21 on cell proliferation, migration and apoptosis of tumors cells [4–7]. In addition, several studies have also demonstrated that miR-21 regulates the expression of Th17 and Treg cells [8,9], indicating the immune regulatory role of miR-21. In addition, miR-21 was also shown to suppress the innate immune response at the early stage after injury [10]. However, the roles of miR-21 in wound healing remain unclear. MiR-21 was upregulated after injury and could promote early wound contraction and migration of keratinocytes by targeting PTEN [11–13]. These results indicated that miR-21 had a strong impact on wound

* Corresponding authors.

E-mail addresses: 13701131933@139.com (H. Wang), lililiuyi@163.com (Y. Liu).

<https://doi.org/10.1016/j.yexcr.2017.11.019>

Received 24 August 2017; Received in revised form 12 November 2017; Accepted 13 November 2017
0014-4827/ © 2017 Elsevier Inc. All rights reserved.

healing, but the specific role of miR-21 in ECM synthesis and the regulatory mechanism require further investigation.

The ECM is the architectural support for tissues, and it also regulates cell proliferation, migration, protein synthesis and degradation, suggesting it plays an important role in the wound repair process [14]. Wound healing is controlled by numerous cell signaling pathways, including the Transforming growth factor (TGF- β) pathway. TGF- β belongs to the TGF- β superfamily and has crucial roles in tissue development and differentiation of vertebrates, control of the immunological response and tissue repair [15]. Smad proteins are mediators of TGF- β signaling and have a major role in the regulation of ECM synthesis and deposition.

In the present study, we found that miR-21 deficiency decreased the ECM deposition and delayed the wound healing process in palate soft tissue. Furthermore, we demonstrated that miR-21 targeted the key inhibitory protein Smad7 and promoted the wound healing process via the Smad7-Smad2/3-Elastin pathway. Our results suggest an effective therapeutic strategy to promote soft tissue healing in the clinic.

2. Materials and methods

2.1. Animals

Five-week old female C57BL/6 J and miR-21-KO mice were purchased from Vital River (Beijing, China) and housed in separate pathogen-free animal facilities under controlled temperature (25 °C) and photoperiods (12:12-h light: dark cycle) and fed a standard diet and tap water. This study was conducted following the approved guidelines established by the Animal Ethics Committee of the School of Stomatology, Capital Medical University (Beijing, China). All animal experiments were performed under the institutionally approved protocols for the use of animals in research (Capital Medical University #2012-x-53).

2.2. Chemicals and antibodies

Unconjugated anti-CD44, anti-CD45, anti-CD146, anti-collagen III and horseradish peroxidase-conjugated anti-rabbit or anti-mouse IgG were purchased from Abcam (San Francisco, CA, USA). Anti-Smad7, anti-Elastin and anti-HSP90 were purchased from Santa Cruz (Dallas, TX, USA). Unconjugated anti-Smad2/3, anti-phospho-Smad2/3, anti-rat IgG-Alexa Fluor 488 antibody and anti-rat IgG-Alexa Fluor 595 antibodies were purchased from Cell Signaling Technology (Danvers, MA, USA).

2.3. Cell culture

Healthy gingival tissues were obtained from WT and miR-21-KO mice, minced and digested in a solution of 3 mg/ml collagenase type I (Sigma-Aldrich) and 4 mg/ml dispase (Sigma-Aldrich) for 30 min at 37 °C. A single cell suspension of all nuclear cells was obtained by passing all bone marrow cells through a 70- μ m strainer (BD Bioscience). The cells were seeded onto 10-cm culture dishes with cell culture medium that contained 20% FBS, 2 mM L-glutamine (Invitrogen), 100 U/ml penicillin and 100 μ g/ml streptomycin (Invitrogen) and incubated at 37 °C and 5% CO₂ in a humidified environment. For each experiment, all primary cells used in this study were at passage 2.

2.4. Wound-healing mouse model

WT and miR21-KO mice (n=5, body weights of 20–22 g) were anesthetized with 1% pentobarbital (30 mg/kg). For the wound model of mouth mucosa, the full-thickness palate ranging from the mesial edge of the second molar to the distal edge of the third molar was removed. The mice were sacrificed after 7 days, and the defect area in palates was observed by stereomicroscopy and assessed using ImageJ.

Then, the palates were fixed with 4% formalin, decalcified with buffered 10% EDTA (pH 8.0), and embedded in paraffin. Sections were deparaffinized and stained with H&E and immunohistochemistry staining.

2.5. Immunocytofluorescence staining

Colonies of GMSCs were harvested on glass coverslips, fixed in 4% paraformaldehyde, blocked in the appropriate normal serum matched to secondary antibodies (10% solution), and incubated with the isotype-matched antibodies overnight at 4 °C. The samples were then incubated with rhodamine/FITC-conjugated secondary antibodies (1:200; Cell Signaling Technology) and mounted using a Vectashield mounting medium containing 4',6-diamidino-2-phenylindole (DAPI) (Sigma-Aldrich) for immunochemical staining. The images were captured using a fluorescence microscope (OLYMPUS, Tokyo, Japan).

2.6. Flow cytometric analysis

GMSCs were harvested and fixed with 80% methanol. The permeabilized cells were incubated in PBS containing 10% normal goat serum and 0.3 M glycine to block non-specific protein binding sites. For phenotypic identification, the cells were incubated with primary anti-CD44, anti-CD146 and anti-CD45 antibodies (Abcam, 1 μ g/10⁶ cells). The secondary antibodies were PE goat anti-mouse IgG and goat anti-rabbit IgG. (Cell Signaling Technology, 1 μ g/10⁶ cells). Cell preparations were immediately analyzed using flow cytometry (FACSCalibur, BD Bioscience). These experiments were performed at 4 °C in the dark.

2.7. Reverse transcriptase polymerase chain reaction (RT-PCR)

Total RNA was extracted from GMSCs of WT and miR21-KO mice using TRIzol reagent (Invitrogen). Then, according to the manufacturer's instructions (Invitrogen), 2 μ g aliquots of RNA were synthesized using random hexamers or oligo (dT) and reverse transcriptase for real-time PCR. The reactions were performed using a QuantiTect SYBR Green PCR kit (Qiagen, Germany) and an iCycler iQ Multi-Color Real-time PCR Detection System. The amplification primer sequences are shown in Table 1.

2.8. Western blot analysis

Total protein of GMSCs and palate tissues was extracted using RIPA buffer (10 mM Tris-HCl, 1 mM EDTA, 1% sodium dodecyl sulfate [SDS], 1% Nonidet P-40, 1:100 proteinase inhibitor cocktail, 50 mM β -glycerophosphate, and 50 mM sodium fluoride). Then, 50–100 μ g of protein was separated on 10% polyacrylamide-SDS gels (Applygen, Beijing,

Table 1
Primers used for RT-PCR.

Gene symbol	Sequence (5'→3')
Mouse Smad7	(F) CGTGCACAGAATTCGAGGAG
	(R) TGGGGAGAAGCAGGCAATTA
Mouse Collagen I	(F) CCTCAGGGTATTGCTGGACA
	(R) GAAGACCAGGGAAGCCTCTT
Mouse Collagen III	(F) CCCAACCCAGAGATCCCATT
	(R) GGTCAACCAATTTCTCCAGGA
Mouse Fibronectin	(F) TACCCCTCCACACCCCAATC
	(R) TGCCAGGAAGCTGAATACCA
Mouse Elastin	(F) AGCCCTAACCCAGAAACTCCC
	(R) CCCCACAAAGAAGAAGCACC
Mouse GAPDH	(F) GAAGATATGGGCACAGGGGA
	(R) CAAGAAGATGCGGCTGTCTC
Mouse Beta-actin	(F) AACAGTCCGCTAGAAGCAC
	(R) CGTTGACATCCGTAAGACC

F: Forward; R: Reverse

Download English Version:

<https://daneshyari.com/en/article/8451480>

Download Persian Version:

<https://daneshyari.com/article/8451480>

[Daneshyari.com](https://daneshyari.com)